Simultaneous ultrafast optical pulse train bursts generation and shaping based on Fourier series developments using superimposed fiber Bragg gratings

Víctor García-Muñoz*, Miguel A. Preciado, and Miguel A. Muriel

ETSI Telecomunicación, Universidad Politécnica de Madrid (UPM), 28040 Madrid, Spain.
**Corresponding author: vicgarmu@gmail.com*

Abstract: We propose an all-fiber method for the generation of ultrafast shaped pulse train bursts from a single pulse based on Fourier Series Developments (FDSs). The implementation of the FSD based filter only requires the use of a very simple non apodized Superimposed Fiber Bragg Grating (S-FBG) for the generation of the Shaped Output Pulse Train Burst (SOPTB). In this approach, the shape, the period and the temporal length of the generated SOPTB have no dependency on the input pulse rate.

OCIS codes: (060.2340) Fiber optics components; (070.6020) Signal processing; (230.1150) All-optical devices; (320.5540) Pulse shaping; (320.7080) Ultrafast devices; (999.9999) Fiber Bragg gratings; (999.9999) Optical pulse generation.

References and links

1. A. M. Weiner, "Femtosecond optical pulse shaping and processing," Prog. Quantum Electron. **19**, 161–235 (1995).
2. J. Azaña, R. Slavík, P. Kockaert, L. R. Chen, and S. LaRochelle, "Generation of customized ultrahigh repetition rate pulse sequences using superimposed fiber Bragg gratings," J. Lightwave. Technol. **21**, 1490-1498 (2003).
3. J. Magné, J. Bolger, M. Rochette, S. LaRochelle, L. R. Chen, B. J. Eggleton, and J. Azaña, "4x100 GHz pulse train generation from a single-wavelength 10 GHz mode-locked laser using superimposed fiber Bragg gratings and nonlinear conversion," IEEE/OSA J. Lightwave. Technol. **24**, 2091-2099 (2006).
4. J. Azaña and M. A. Muriel, "Technique for multiplying the repetition rates of periodic trains of pulses by means of a temporal self-imaging effect in chirped fiber Bragg gratings," Opt. Lett. **24**, 1672-1764 (1999).
5. P. Petropoulos, M. Ibsen, A. D. Ellis, D. J. Richardson, "Rectangular pulse generation based on pulse reshaping using a superstructured fiber Bragg grating," IEEE/OSA J. Lightwave Technol. **19**, 746-752 (2001).
6. N. K. Berger, B. Levit, aand B. Fischer, "Reshaping periodic light pulses using cascaded uniform fiber Bragg gratings," J. Lightwave Technol. **24**, 2746- 2751 (2006).
7. J. Azaña and L. R. Chen, "Synthesis of temporal optical waveforms by fiber Bragg gratings: a new approach based on space-to-frequency-to-time mapping," J. Opt. Soc. Am. B **19**, 2758-2769 (2002).
8. I. Littler, M. Rochette, and B. Eggleton, "Adjustable bandwidth dispersionless bandpass FBG optical filter," Opt. Express **13**, 3397-3407 (2005).
9. M. A. Preciado, V. García-Muñoz, and M. A. Muriel "Grating design of oppositely chirped FBGs for pulse shaping," IEEE Photon. Technol. Lett. **19,** 435-437 (2007).
10. S. Longhi, M. Marano, P. Laporta, O. Svelto, "Propagation, manipulation, and control of picosecond optical pulses at 1.5 μm in fiber Bragg gratings," J. Opt. Soc. Am. B **19**, 2742-2757 (2002).
11. J. A. Bolger, I. C. M. Littler and B. J. Eggleton, "Optimisation of superimposed chirped fibre Bragg gratings for the generation of ultra-high speed optical pulse bursts," Opt. Commun. **271**, 524-531 (2007).
12. T. Erdogan, "Fiber Grating Spectra," IEEE/OSA J. Lightwave Technol. **15**, 1277-1294 (1997).

1. Introduction

All-optical approaches for the reshaping and the generation of ultrafast optical pulse trains have a great interest in optical communications, in device characterization and in other applications [1]. The achievement of shaped high repetition rate pulses would be desirable for

#84990 - $15.00 USD Received 6 Jul 2007; revised 13 Aug 2007; accepted 13 Aug 2007; published 14 Aug 2007

several optical communications applications, such as the generation of ultrafast clock signals for optical switching in ultradense optical time-division multiplexing systems.

The generation of ultra high speed pulse train bursts using S-FBGs composed by identical non apodized FBGs with slightly displaced central frequency has been previously demonstrated by Azaña *et al*. [2]. In this scheme the obtained pulse train has a period equal to the inverse of the frequency separation of the individual FBGs that form the S-FBG. The overall temporal envelope of the pulse train corresponds to the reflective impulse response of an individual FBG. When pulse rate multiplication is desired, the generated pulse train total duration is matched to the pulse rate of the signal arriving to the filter. The achievement of pulse train burst with no pulse to pulse amplitude variation requires the overall temporal envelope to be squared. Squared overall temporal envelopes can be obtained with uniform FBGs in the weak reflectivity regime (reflectivity about 15%) and with Linearly Chirped Fiber Bragg Gratings (LCFBGs) in the moderate reflectivity regime (reflectivity about 20%). The limitation imposed by pulse to pulse phase fluctuations of the obtained pulse train can be overcame by using nonlinear optical mirrors [3], which also provide the advantage of the generation of multiwavelength pulse trains. LCFBGs have also been used for multiplying the repetition rate of a periodic pulse train [4] by means of the Talbot effect. In this technique the dispersion of the filter is chosen to accomplish the Talbot condition in which the incident pulse train is replicated at a higher repetition rate. This technique is only applicable over periodical sequences of identical pulses, i.e. with the same phase and intensity. Moreover, very long gratings are usually needed. Regarding pulse shaping, several in fiber approaches have been presented with uniform FBGs such as the Born approximation (weak reflectivity regime) [5]. Concatenated uniform FBGs [6] can also be deployed, but low reflectivity and periodic input signal are imposed. Highly dispersive LCFBGs with moderate reflectivity have been deployed for pulse shaping [7-9]. An approach for simultaneous pulse rate multiplication and reshaping using apodized LCFBGs was proposed by Longhi *et al*. [10]. In this scheme, the Talbot condition over the dispersion is normally higher enough to accomplish the space-to-frequency mapping condition, then simultaneous pulse shaping and multiplication can be achieved, but complicated apodization and very long gratings are required.

The possibility of tailoring the shape of the individual pulses of the generated pulse burst obtained with a S-FBGs have been pointed out previously [2,11] but, up to our knowledge, no studies have been done in order to obtain such type of filters. The approach presented in this paper proposes the use of short, non apodized S-FBGs to perform a FSD for the generation of pulse train burst in which the individual pulses of the pulse train are shaped. The reflectivity and the global phase of each grating are designed so as to match the values of the FSD of the desired pulse. Besides all the advantages of all-fiber systems such as low cost and low insertion loss, this approach will provide compactness and easy to construct advantages owing to the non apodization and the absence of phase shifts inside each FBG. In addition, the desired shaped pulse burst can be generated form a single pulse contrarily to the Talbot based approach in which the input signal must be periodic.

The reminder of this paper is organized as follows. In section 2, we describe the theoretical basis of our new technique for simultaneous pulse shaping and multiplication based on FSD. In the two following sections, we describe the grating design equations for the cases where FSD are implemented with Bragg gratings: the case using Uniform S-FBGs, and the case using superimposed LCFBGs (S-LCFBGs). After describing the grating design equations, we present some simulation examples that confirm the predictions made in the previous sections. Finally, conclusions from this study are drawn.

2. Theory

Let us consider a filter composed by the sum of several individual filters. We suppose that each individual filter consists of a replica of a band-pass filter displaced in frequency and multiplied by a different complex number c_p. The frequency response of the whole filter can be expressed as

#84990 - $15.00 USD Received 6 Jul 2007; revised 13 Aug 2007; accepted 13 Aug 2007; published 14 Aug 2007

$$H(\omega)=\sum_{p=-p_{\min}}^{p_{\max}} H_p(\omega)=\sum_{p=-p_{\min}}^{p_{\max}} c_p H_0(\omega-p\Delta\omega) \tag{1}$$

where $H_p(\omega)$ is the *pth* individual filter and $H_0(\omega)$ is defined as the generator filter with bandwidth $\delta\omega$. The frequency separation between the individual filters is set by $\Delta\omega$. The sum ranges from $-p_{min}$ to p_{max} where p_{min} and p_{max} are integer numbers. The number of replicated filters is $M = p_{\min} + p_{\max} + 1$. The frequency ω corresponds to the base band frequency, i.e. $\omega=\omega_{opt}-\omega_0$, where ω_{opt} is the optical frequency and ω_0 is the central optical frequency of the whole filter. The corresponding complex envelope impulse response is:

$$h(t)=h_0(t)\sum_{p=-p_{\min}}^{p_{\max}} c_p \exp(jp\Delta\omega t) \tag{2}$$

The impulse response is composed by two terms. The first term $h_0(t)$ is the impulse response of the generator filter $H_0(\omega)$ and acts as overall temporal envelope, hence the SOPTB duration t_h is set by the duration of $h_0(t)$. The shape of $h_0(t)$ has to be squared in order to avoid pulse to pulse amplitude variations. The second term consists of an *M* elements sum of complex numbers multiplied by frequency equispaced complex exponentials. This second term acts as pulse shaper of the individual pulses forming the output signal.

The temporal response complex envelope $y(t)$ of the whole filter to a temporal input pulse with complex envelope $x(t)$ is given by the convolution of the impulse response of the whole filter with the input pulse.

$$y(t)=h(t)*x(t) \tag{3}$$

In the frequency domain, the spectral response of the filter $Y(\omega)$ is equal to the product of the input pulse spectrum $X(\omega)$ with the spectral response of the filter $H(\omega)$.

$$Y(\omega)=H(\omega)X(\omega) \tag{4}$$

The output temporal signal $y(t)$ can be approximated to the impulse response when the input pulse spectrum $X(\omega)$ is considered flat all over the filter bandwidth, that is,

$$y(t)=h_0(t)s\sum_{p=-p_{\min}}^{p_{\max}} c_p \exp(jp\Delta\omega t) \tag{5}$$

where *s* is a complex constant of proportionality. Under this assumption, provided that the shape of $h_0(t)$ is flat and the set of complex numbers c_p coincide with the coefficients of a FSD with fundamental harmonic set by $\Delta\omega$, the input signal can be reshaped to any desired form with repetition period $T=2\pi/\Delta\omega$. Equation (5) only applies when the input pulse spectrum $X(\omega)$ can be considered flat all over the whole filter bandwidth. This consideration limits the filter bandwidth to the frequency range where the input spectrum can be considered as flat. A limited filter bandwidth reduces the number of individual filters that can be implemented. In other words, a limited filter bandwidth limits the number of harmonics of the FSD. A reduction on the number of harmonics leads to a less accurate shaping of the individual pulses that compose the SOPTB.

In our approach, a better use of the available bandwidth is reached when the spectrum of the input pulse can be considered flat just over the bandwidth $\delta\omega$ of the generator filter $H_0(\omega)$. That is, if the input pulse spectrum $X(\omega)$ can be considered flat just over the bandwidth of each individual filter $H_p(\omega)$ that form the whole filter, then the output frequency response $Y(\omega)$ can be expressed as

$$Y(\omega)=\sum_{p=-p_{\min}}^{p_{\max}} X_p c_p H_0(\omega-p\Delta\omega) \tag{6}$$

where the factors X_p can be chosen as samples of $X(\omega)$, $X_p=X(p\Delta\omega)$ or by energetic reasons in a way that the approximated function has the same total energy that the function to be approximated. In the temporal domain, the complex envelope of the temporal response has the form

#84990 - $15.00 USD Received 6 Jul 2007; revised 13 Aug 2007; accepted 13 Aug 2007; published 14 Aug 2007

$$y(t) = h_0(t) \sum_{p=-p_{\min}}^{p_{\max}} X_p c_p \exp(jp\Delta\omega t) \tag{7}$$

This approximation permits to perform the FSD with a better exploitation of the input signal bandwidth just matching the set of complex numbers $d_p = X_p c_p$ with the coefficients of the FSD with fundamental harmonic $\Delta\omega$ of the desired SOPTB ($y(t)$).

The maximum reflectivity of each *pth* individual filter $R_{p,\max}$ that forms the whole filter is defined as

$$R_{p,\max} = \max\left(\left|H_p(\omega)\right|^2\right) = \left|c_p\right|^2 \max\left(\left|H_0(\omega)\right|^2\right) \tag{8}$$

In this approach, $R_{p,\max}$ is related to the FSD coefficients d_p of the desired SOPTB, the maximum reflectivity of the generator filter $R_{0,\max} = \max\left(\left|H_0(\omega)\right|^2\right)$ and the values of the input pulse spectrum samples X_p

$$R_{p,\max} = \left|\left(d_p / X_p\right)\right|^2 R_{0,\max} \tag{9}$$

If the norm of the set of complex numbers c_p is normalized to the unity, the maximum reflectivity of the whole filter corresponds to the maximum reflectivity of the generator filter.

The global phase φ_p of the *pth* individual filter spectral response is determined by the phase of the complex number $c_p = d_p / X_p$.

S-FBS are very suitable devices for the physical realization of multiband filters with no temporal delay among the individual reflected bands. Two possibilities have been previously reported [7] for the implementation of non apodized multiband filters with temporal flat response: the use of uniform S-FBG and the use of S-LCFBGs. The use of S-LCFBGs technique (Fig. 1) is only applicable for pulse intensity shaping, since the SOPTB is chirped.

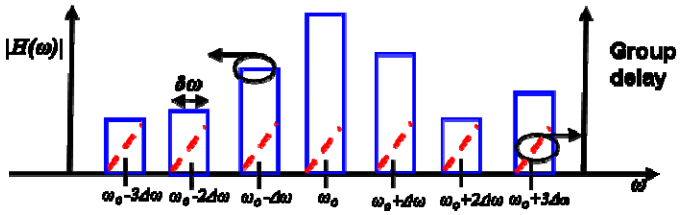

Fig. 1. (color online) Schematic diagram of the pulse shaper with chirped filters. Amplitude response (blue) and group delay (red). In the case where uniform filters are used, the group delay remains constant.

The number of elements of the FSD equals the number of generator filters that form the frequency response, hence the higher the number of generator filters, the better the development. Notice that for the previous methods [5, 9, 10] the frequency response is truncated, which is similar to limit the number of elements of a FSD. The limitation of the number of generator filters can be caused by two reasons, the available bandwidth and the refractive index saturation of the fiber produced by the consecutive inscriptions in the fabrication of S-FBGs.

3. Grating design for FSD filters based on Uniform S-FBGs

The generation of shaped pulses using supersructured FBGs in the weak grating limit has been previously reported [5]. The use of superstructured FBGs is necessary when the input pulse spectrum can not be taken as flat all along the filter bandwidth. For the generation of a

#84990 - $15.00 USD Received 6 Jul 2007; revised 13 Aug 2007; accepted 13 Aug 2007; published 14 Aug 2007

SOPTB a concatenation of superstructured FBGs can be performed, but it yields to a very complicated apodized structure. Then, it would be interesting to have simpler structures to obtain SOPTB which contains several pulses. In this section we develop the required basis to obtain the appropriate conditions and make a precise design of uniform S-FBGs that provide the generation of SOPTB.

The refractive index (RI) profile of a uniform S-FBG follows the expression

$$n(z) = n_{av} + \sum_{p=-p_{\min}}^{p_{\max}} \Delta n_p \cos\left(\frac{2\pi}{\Lambda_{0p}} z + \varphi_p\right) \qquad \text{-L/2} \le \text{z} \le \text{L/2} \tag{10}$$

where the sum extends over the M Bragg gratings inscribed, n_{av} is the average RI, L is the perturbation length; Δn_p, Λ_{0p} and φ_p are, respectively, the maximum RI modulation, the grating period and the global phase of the *pth* Bragg grating inscription. The grating period determines the central frequency of each individual filter

$$\Lambda_{0p} = \frac{\pi c}{n_{av}(\omega_0 + p\Delta\omega)} \tag{11}$$

where ω_0 is the central optical frequency of the filter. The grating length is obtained from the SOPTB temporal length t_h, $L = (c/2n_{av})t_h$, where c is the vacuum speed of light, since we consider that the electric field crosses the entire device. In the weak grating limit [12] the *pth* index modulation follows the expression

$$\Delta n_p = \frac{2c}{L(\omega_0 + p\Delta\omega)} \operatorname{atanh}\left(\sqrt{R_{p,\max}}\right) \tag{12}$$

where $R_{p,max}$ is calculated using Eq. (9). The global phase φ_p of the RI is directly related to the phase of the FSD elements; note that no intermediate phase shifts are needed in this approach. The number of generator filters of the filter is only limited by the photosensibility of the fiber and the available bandwidth given by the input pulse; nevertheless the weak reflectivity of the uniform FBGs that form the filter ensures that the saturation of the fiber is not attained.

This approach permits to perform the generation of SOPTBs with no lower limit on its total temporal pulse train duration t_h. We can generate a pulse train bursts with only one pulse just making coincide the pulse train duration t_h with the FSD period. However, there is an upper limit on the SOPTB duration related to the limits of the Born approximation. The Born approximation is accomplished when the product κL is very low. The factor κ is the coupling coefficient and it is proportional to the RI modulation. The minimal fabrication limit for the induced RI modulation is set to 10^{-5} [7]. This fabrication limit leads to a maximum grating length of the order of several cm. For lengths greater than this maximum, the Born approximation is not attained. This fact imposes a maximum limit of the SOPTB duration of the order of a hundred of ps since the S-FBG maximal length is limited to a few cm.

4. Grating design for FSD filters based on S-LCFBGs

The generation of a SOPTB could be carried out by applying the space-to-frequency-to-time mapping approximation [7] with concatenated LCFBGs. However, this approach is only applicable to individual shaped pulse durations in the range of tens of picoseconds, even for input pulses in the picosecond or subpicosecond regime. Hence, for the applications where the pulses involved are of the order of few picoseconds other approaches are necessary.

In this section we derive the conditions over the parameters of a S-LCFBG in the moderate reflectivity regime for the generation of shaped pulse trains with squared overall temporal envelope in the FSD based filters scheme.

The RI profile of a non apodized S-LCFBG follows the expression

#84990 - $15.00 USD Received 6 Jul 2007; revised 13 Aug 2007; accepted 13 Aug 2007; published 14 Aug 2007

$$n(z) = n_{av} + \sum_{p=-p_{\min}}^{p_{\max}} \Delta n_p \cos\left(\frac{2\pi}{\Lambda_{0p}} z + \frac{C_{Kp}}{2} z^2 + \varphi_p \right) \quad \text{-L/2} \le \text{z} \le \text{L/2} \tag{13}$$

where C_{Kp} is the chirp factor of the *pth* Bragg grating inscription and the rest of parameters are defined in the former section. The S-LCFBG length and the grating period for each grating are obtained with the expressions given in the former section. The global phase φ_p of the RI is directly related to the phase of the FSD elements.

As stated before, the filter is formed by replicas of the generator filter. The only difference between the individual filters $H_p(\omega)$ is the reflectivity, the global phase and the central frequency of each filter. Consequently all the individual filters should have the same bandwidth and the same dispersion $\ddot{\phi}$. For a given length, the filter bandwidth sets the chirp factor [9]; then, the chirp factor is equal for all the filters and follows the expression

$$C_K = -4n_{av}^2 \delta\omega / (c^2 t_h) \tag{14}$$

In the high dispersion and moderate reflectivity regime, the impulse response temporal shape of a non apodized LCFBG is squared. The condition of high dispersion regime can be expressed as [10]

$$\left|\ddot{\phi}\right| \gg 1/\delta\omega^2 \tag{15}$$

where $\delta\omega$ is the generator filter bandwidth. On the other hand, the dispersion is related to the SOPTB duration and the generator filter bandwidth.

$$\left|\ddot{\phi}\right| = t_h / \delta\omega \tag{16}$$

From Eq. (15) and Eq. (16) we deduce that $t_h \gg 1/\delta\omega$. The frequency separation $\Delta\omega$ is lower than the bandwidth of the generator filter $\delta\omega$ to avoid frequency overlapping between the individual filters. The frequency overlapping causes ripples in the amplitude and in the group delay of the frequency response. These ripples lead to a decrease of the filter energetic efficiency and to an increase of the pulse to pulse amplitude variations in the SOPTB temporal amplitude envelope [4]. Our simulations show that, even for a 30% frequency overlapping of the individual filters bands, the pulse to pulse amplitude variations are lower than 15 %. In order to obtain a maximal energetic efficiency and minimal pulse to pulse amplitude variations, the generator filter bandwidth $\delta\omega$ should be equal to the frequency separation $\Delta\omega$. Then, for the case of maximal energetic efficiency, a condition which relates the SOPTB duration with the period of the SOPTB is obtained

$$t_h \gg T / 2\pi \tag{17}$$

Our simulations have shown that the high dispersion condition is reached for SOPTB with five or more periods.

For LCFBGs under the high dispersion and moderate reflectivity regime the index modulations follow the expression [9].

$$\Delta n_p = \frac{2n_{av}}{(\omega_0 + p\Delta\omega)} \sqrt{-\frac{2}{\pi\left|\ddot{\phi}\right|} \ln\left(1 - R_{p,\max}\right)} \tag{18}$$

where, as in the former case, ω_0 is the central optical frequency of the whole filter and $R_{p,max}$ is calculated using Eq. (9).

It is worth noting that in the weak grating limit, the Born approximation also applies for S-LCFBGs with no condition over the dispersion. In this case the S-FBG is chirped in order to

#84990 - $15.00 USD Received 6 Jul 2007; revised 13 Aug 2007; accepted 13 Aug 2007; published 14 Aug 2007

obtain a better energetic efficiency than in the not chirped one. The only condition over the dispersion is that the bandwidth enlargement produced by the grating chirp must not provide a large overlapping of the generator filter bandwidth in order to avoid a decrease of the energetic efficiency and an increase of the pulse to pulse amplitude variations.

5. Examples and results

In this section we present numerical simulations that confirm the theoretical results presented above. We demonstrate the generation of SOPTBs with individual pulse width of the order of the input pulse width since the filter bandwidth is comparable with the input pulse bandwidth. For all the examples, we assume a gaussian input pulse with a t_{FHWH} of 0.5 ps and a carrier frequency $\omega_0/(2\pi)$ of 193 THz. The temporal length of the SOTPB and its period are set to 40 ps and 4 ps respectively. The frequency separation of the individual filters is 250 GHz, but in the regions where the FSD coefficients are null the separation is greater. The length of all the gratings is 4.12 mm and the effective refractive index of the optical fiber is 1.452.

5.1 FSD filters based on Uniform S-FBGs

In this subsection the generation of a non chirped SOPTB consisting of 10 squared pulses with pulse width of 2 ps and a period of 4 ps is presented.
The FSD not null coefficients of a square pulse signal are

$$d_p = \begin{cases} -j/(p\pi) & p\ odd \\ 1/2 & p = 0 \end{cases} \tag{19}$$

In Fig. 2(a) we can see the frequency amplitude response of the superposition of nine uniform FBGs where the maximum reflectivity was set by design to 12% so as to ensure a flat top overall envelope. The obtained amplitude response corresponds to a sequence of sinc-like functions. The amplitude variations in the lateral lobes of the sincs are due to the approximation of the input pulse shape by a step function. We can see in the calculated amplitude response that the maximum reflectivity is not in the center of the spectrum. Owing to the small value of the input spectrum in the tails of the bandwidth, the reflectivity of the filter in the tails should be maximal in order to take into account the contributions of the higher order FSD terms. Consequently, a reduction of energetic efficiency is produced, but an increase of accuracy in the development is reached.

In Fig. 2(b) we can see the temporal envelope of a SOPTB with ten pulses, pulse width 2 ps and a 10-90% rise/fall time of 0.25 ps with an amplitude variation across the top of each pulse from 5% for the middle pulses and 15% for the first and the last pulse. The amplitude variations present all over the SOTPB duration are due to the well known Gibbs phenomenon and are unavoidable since the FSD has a finite number of terms. The temporal sharp peaks present in the beginning and in the end of the SOTPB are due to the reflections in the limits of the gratings caused by the difference between the RI of the fiber and the average RI of the S-FBG. We also observe that the pulse to pulse amplitude variations are marginal as the overall envelope is flat top.

In this case, the total amount of RI modulation is about 1.969×10^{-4}, which does not achieve RI saturation. The minimal RI modulation for this example is 1.3×10^{-5} which is greater than the minimum RI achievable. The energetic efficiency, defined as the quotient between the input and the output signal energy, is about 0.31%; hence in most cases an amplificator should be placed after the pulse shaper.

Note that the spectral response of the output signal obtained with a superstructured FBG [5] would be identical to the one obtained with our approach since no chirp is applied to the period of the FBGs that form the whole filter. Consequently, the energetic efficiency has the same value in both cases, but the use of FSD avoids complicated apodization and reduces drastically the number of phase shifts.

#84990 - $15.00 USD Received 6 Jul 2007; revised 13 Aug 2007; accepted 13 Aug 2007; published 14 Aug 2007

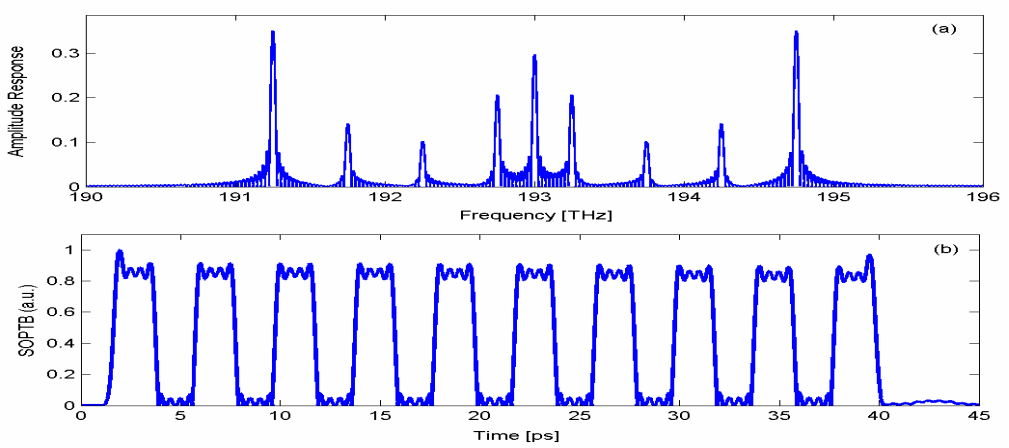

Fig. 2. Generation of a square SOPTB with a uniform S-FBG. (a) Amplitude response of the filter. (b) Temporal amplitude envelope of the SOPTB.

5.2 FSD filters based on S-LCFBGs

In this subsection, in addition to the simulations that confirm the theory described in this paper, we present a suitable election of the corresponding FSD elements so as to obtain energetically efficient filters when only the magnitude of the output pulse shape is specified. Design criteria are presented for the cases of rectangular pulses with duty cycle equal to ½. In the two examples of this subsection, the maximum reflectivity is set to 20%. In both examples, the generator filter bandwidth is set to 250 GHz. The FWHM input signal bandwidth is 1.7651 THz and its total bandwidth is greater than 4 THz, this bandwidth is more than 16 times greater than the generator filter bandwidth. Therefore, the input signal bandwidth $X(\omega)$ can be considered constant over each individual filter bandwidth and the approximation presented in Eq. (6) applies.

In the first example (Fig. 3), the FSD of a squared signal with a pulse width of 2 ps and a period of 4 ps is presented. The FSD coefficients are the same that in the former case.

In Fig. 3(a) we show the calculated amplitude response of the grating. We observe that, as in the former case, the maximum reflectivity is not in the center of the spectrum. We can also see a slightly frequency overlapping in the central bands of the amplitude response that will not affect the shape of the generated SOPTB. Fig. 3(b) shows the group delay, which is linear and ranges from zero to the duration of the SOTPB in each individual LCFBG.

In Fig. 3(c) we can see the temporal amplitude envelope of the SOPTB with ten pulses, pulse width 2 ps and a 10-90% rise/fall time of 0.3 ps. The first pulse presents a sharp peak caused by the difference between the RI of the fiber and the average RI of the S-FBG at the beginning of the S-LCFBG. The peak related with the RI difference between RI of the fiber and the average RI of the S-FBG at the end of the S-LCFBG lies at the end of the SOTPB and it is indistinguishable from the Gibbs related ripples present all over the SOPTB. The amplitude variation across the top of each pulse goes from 10% for the first pulses to 15% for the last pulses of the SOPTB. We can also observe a 5% pulse to pulse amplitude variation. This pulse to pulse amplitude variation is caused because the overall envelope is not perfectly flat top.

The frequency response of the individual filters that form the pulse shaper obtained with S-LCFBGs is squared, in contrast with the sinc shaped frequency responses obtained with uniform S-FBGs. This fact, in addition to the fact that the maximum reflectivity can be greater for S-LCFBGs yields to a major energetic efficiency of the filter. When using S-LCFBGs the pulse amplitude variations are greater and the pulses are chirped, but they provide an energetic efficiency ten times greater (4.5%) than in the case where a uniform S-FBG is used.

#84990 - $15.00 USD Received 6 Jul 2007; revised 13 Aug 2007; accepted 13 Aug 2007; published 14 Aug 2007

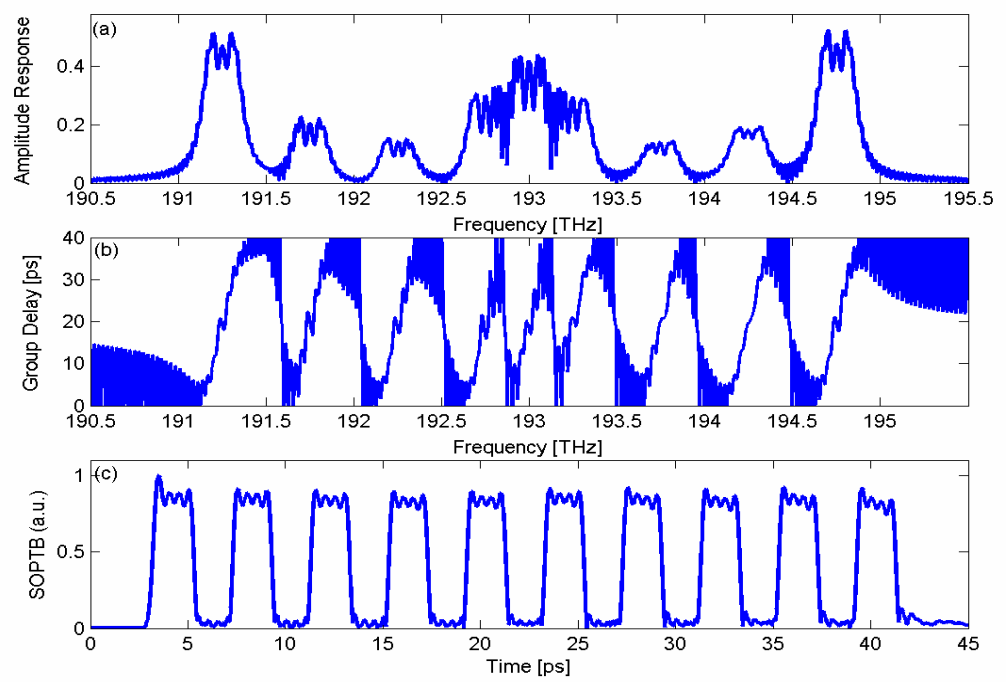

Fig. 3. Generation of a square SOPTB with S-LCFBG considering dc term. (a) Amplitude Response of the filter. (b) Group Delay. (c) Temporal amplitude envelope of the SOPTB.

In the next example, in order to have a better exploitation of the available bandwidth, the FSD of a periodic asymmetrical square pulse signal with a period of 8 ps, which corresponds to a period of 4 ps in amplitude, has been performed. The not null FSD coefficients of an asymmetrical square pulse signal are

$$d_p = \frac{j}{p\pi}\left(\cos\left(p\pi/4\right) - \cos\left(p3\pi/4\right)\right) \quad p\ odd \tag{20}$$

Notice that the frequency separation between the individual LCFBGs would be reduced to 125GHz but, as the zero (dc term) and all the even order coefficients of the FSD are null, the actual frequency separation is 250 GHz. Therefore the bandwidth of the generator filter can be enlarged to 250 GHZ providing a total exploitation of the available bandwidth. In Fig. 4(a) we can see that there are not zones with zero reflectivity in the amplitude response of the filter that implements the FSD of an asymmetric squared SOPTB.

Figure 4(c) shows the temporal amplitude envelope of the SOPTB, with ten pulses, pulse width 2 ps and a 10-90% rise/fall time of 0.3 ps. The amplitude variation across the top of each pulse goes from 7% for the first pulses to 18% for the last pulses of the SOPTB. The pulse to pulse amplitude variation is the same that in the former case since we have used the same generator filter with the same maximum reflectivity that provides the same overall amplitude envelope. For this example without dc term, the energetic efficiency is 8.5%. The SOPTB obtained has similar characteristics that for the previous example, but with an increased energetic efficiency by a factor two with respect to the case with dc term.

#84990 - $15.00 USD Received 6 Jul 2007; revised 13 Aug 2007; accepted 13 Aug 2007; published 14 Aug 2007

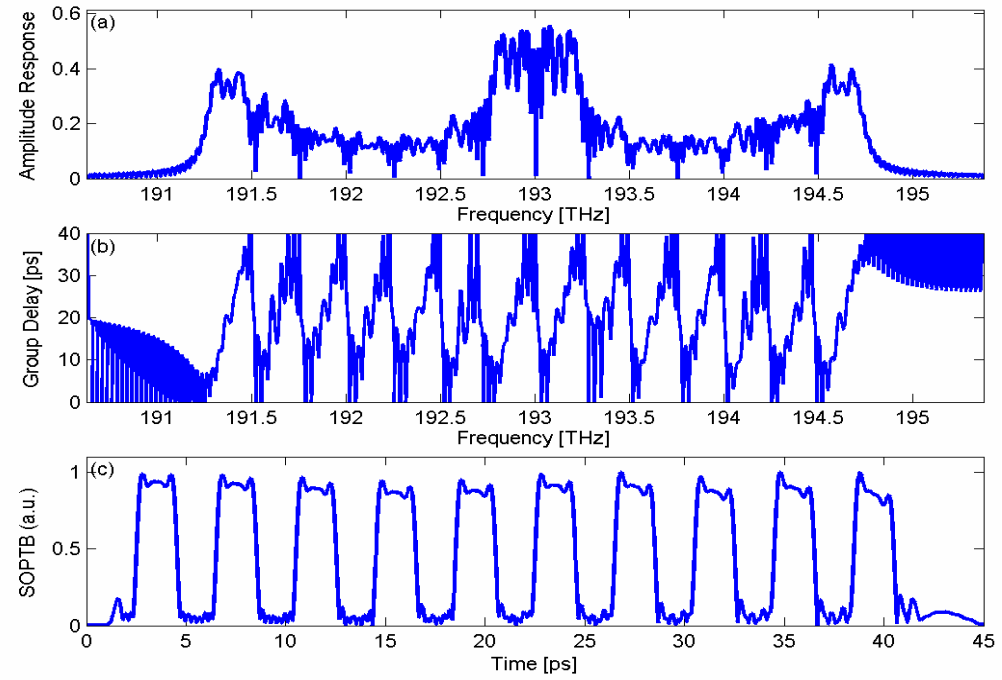

Fig. 4. Generation of a square SOPTB with S-LCFBG without dc term. (a) Amplitude response of the filter. (b) Group delay. (c) Temporal amplitude envelope of the SOPTB.

The main drawback of the filter without dc term is that the required number of fiber illuminations is almost doubled for a given available bandwidth, but, as stated before, in the moderate reflectivity regime core fiber RI saturation is not likely to happen. In this example, the total amount of RI modulation was about 1.52×10^{-3} which does not achieve RI saturation. Additionally, the total amount of RI modulation can be reduced simply by reducing the reflectivity of the generator filter. This reduction of reflectivity avoids index saturation and produces a flatter overall impulse response. The only drawback of the reduction of the reflectivity is that the energetic efficiency decreases, but it continues to be much greater than for the case with dc term.

5.4 Tolerance Analysis

The model developed in the previous sections would not be useful if variations on the S-FBG structure of the filter degrade significantly the shape of the individual pulses of the SOPTB. For the validation of the model against variations in the structure of the S-FBG, we made a study similar to Petropoulos *et al.* [5] in which noisy variations of the amplitude and phase where added to the RI of the Bragg grating filter. We assumed that the variations in phase and in amplitude were independent of each other. We also assumed that the random variations follow a normal distribution. The random variation in amplitude was simulated with a standard deviation of 0.02 and mean value equal to the unity and the variation in phase has a standard deviation of 0.04 and zero mean value. In Fig. 5 we can see that the variations in the SOPTB shape between the ideal filter and the filter with imperfections in its structure are marginal for the three cases presented in the previous sections.

#84990 - $15.00 USD Received 6 Jul 2007; revised 13 Aug 2007; accepted 13 Aug 2007; published 14 Aug 2007

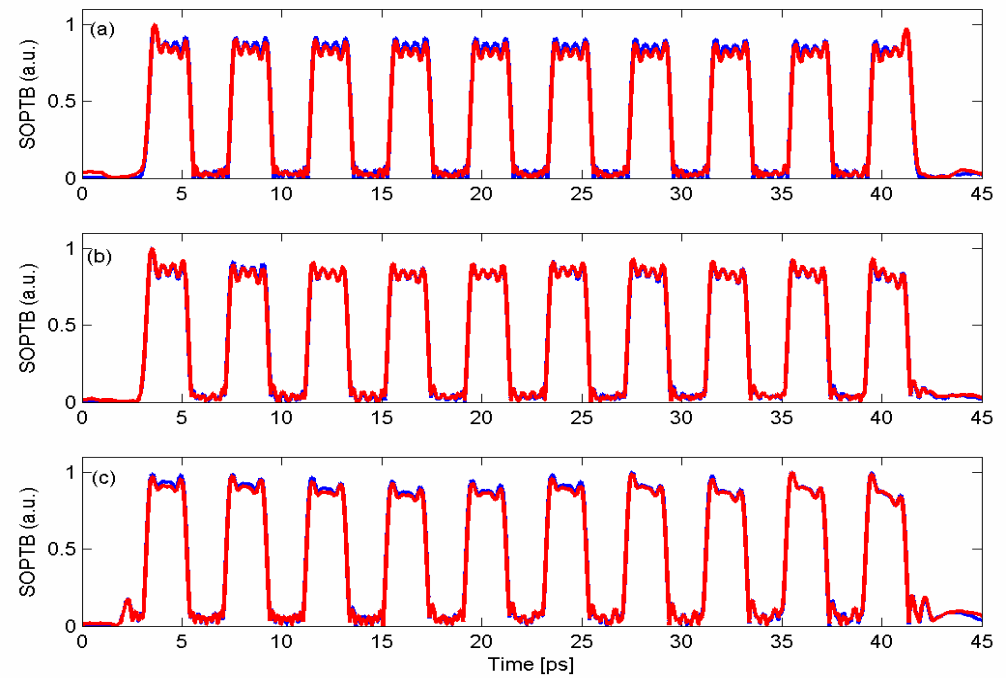

Fig. 5. (color online) Effect of the variations on the S-FBG imperfections in the temporal amplitude envelope of the SOPTB. (a) Uniform S-FBG: ideal structure (blue), noisy structure (red). (b) S-LCFBG with dc term: ideal structure (blue), noisy structure (red). (c) S-LCFBG without dc term: ideal structure (blue), noisy structure (red).

This approach has to be also robust against variations in the input pulse characteristics. Figure 6 shows the SOPTB temporal amplitude envelope for the cases where the input pulse width corresponds exactly to the design width (t_{FWHM} = 0.5 ps) and for the extreme case where the FWHM input pulse width is 0.7 ps, (40% greater than the design width) for the three examples presented in the previous sections. The main effect of this pulse width mismatching is an increase of the 10-90% rise/fall time. The 10-90% rise/fall time increases from 0.3 ps for the ideal case to 0.7 ps for the non-ideal case in the first example (uniform S-FBG) and from 0.25 ps to 0.7 ps in the two other examples (S-LCFBGs) Moreover, no increase of the amplitude variation across the top of each pulse is observed.

#84990 - $15.00 USD Received 6 Jul 2007; revised 13 Aug 2007; accepted 13 Aug 2007; published 14 Aug 2007

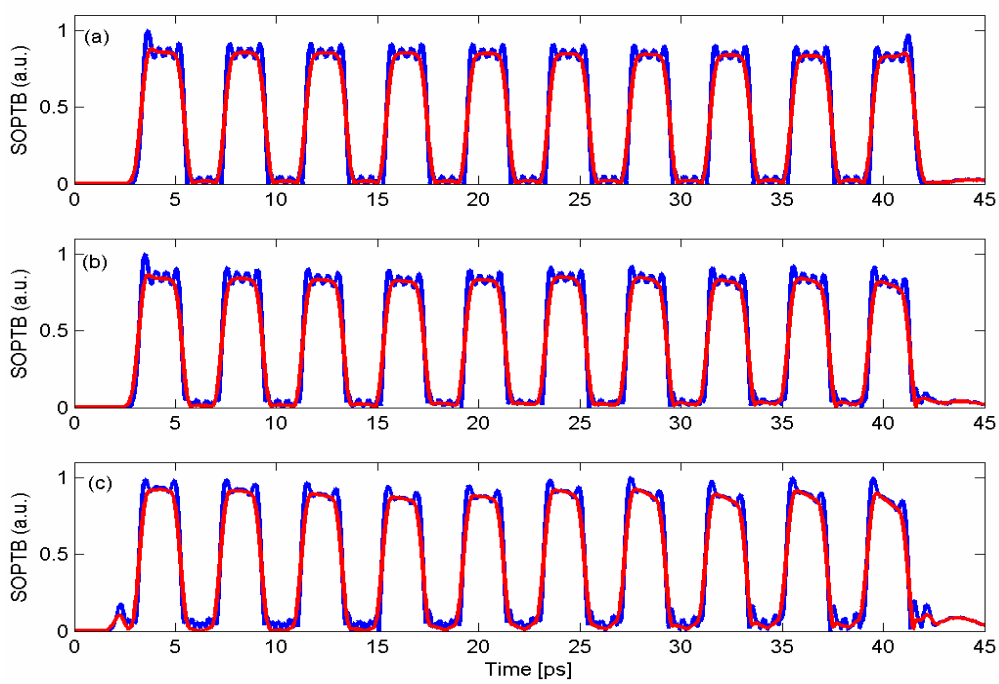

Fig. 6. (color online) Effect of the variations on the input pulse width in the temporal amplitude envelope of the SOPTB. (a) Uniform S-FBG: t_{FWHM} =0.5 ps (blue), t_{FWHM} =0.7 ps (red). (b) S-LCFBG with dc term: t_{FWHM} =0.5 ps (blue), t_{FWHM} =0.7 ps l (red). (c) S-LCFBG without dc term: t_{FWHM} =0.5 ps l (blue), t_{FWHM} =0.7 ps (red)

This analysis of tolerance demonstrates theoretically the robustness of this method in terms of variations of the filter and the input pulse parameters.

6. Conclusion

In this letter we have proposed and numerically simulated a very easy to construct approach for the generation of a shaped ultrafast pulse train burst from a single input pulse. This technique, which is based on the FSD of the desired output pulse shape, only requires a short non apodized S-FBG to be implemented. When the shape of the input pulse is taken into account, provided that the input pulse spectrum can be approximated by a step like function, no apodization of the FBGs that form the filter is needed, contrarily to superstructured FBGs based approaches. This scheme can also provide simultaneous pulse rate multiplication and shaping just matching the SOPTB duration with the period of the input signal.

We have deduced the grating design equations for the cases where uniform S-FBGs are used as FSD filters in the weak grating regime and for S-LCFBG acting in the moderate reflectivity regime. In addition, we have presented an improvement of this technique for square signals with duty cycle equal to ½ that provides a better exploitation of the available bandwidth. Finally, our tolerance analysis shows that this method is robust to variations in the structure of the filter and in the input pulse width.

Acknowledgments

We would like to thank our reviewers for their thoughtful comments and suggestions. This work was supported by the Spanish *Ministerio de Educación y Ciencia* under the projects "Plan Nacional de I+D+I TEC2004-04754-C03-02" and "Plan Nacional de I+D+I TEC2007-68065-C03-02". Víctor García-Muñoz also thanks the support of the *Telecommunications Department, Faculté Polytechnique de Mons*, where he has been a visiting researcher with a grant of the *Consejo Social Universidad Politécnica de Madrid.*

#84990 - $15.00 USD Received 6 Jul 2007; revised 13 Aug 2007; accepted 13 Aug 2007; published 14 Aug 2007